



NRC Publications Archive Archives des publications du CNRC

Synthesis of highly fluorinated poly(arylene ether)s copolymers for proton exchange membrane materials

Kim, Dae Sik; Robertson, Gilles P.; Guiver, Michael D.; Lee, Young Moo

This publication could be one of several versions: author's original, accepted manuscript or the publisher's version. / La version de cette publication peut être l'une des suivantes : la version prépublication de l'auteur, la version acceptée du manuscrit ou la version de l'éditeur.

For the publisher's version, please access the DOI link below. / Pour consulter la version de l'éditeur, utilisez le lien DOI ci-dessous.

Publisher's version / Version de l'éditeur:

<https://doi.org/10.1016/j.memsci.2006.03.020>

Journal of Membrane Science, 281, 1-2, pp. 111-120, 2006

NRC Publications Record / Notice d'Archives des publications de CNRC:

<https://nrc-publications.canada.ca/eng/view/object/?id=c791c99c-71ef-4280-85ed-a3279493a9c3>

<https://publications-cnrc.canada.ca/fra/voir/objet/?id=c791c99c-71ef-4280-85ed-a3279493a9c3>

Access and use of this website and the material on it are subject to the Terms and Conditions set forth at

<https://nrc-publications.canada.ca/eng/copyright>

READ THESE TERMS AND CONDITIONS CAREFULLY BEFORE USING THIS WEBSITE.

L'accès à ce site Web et l'utilisation de son contenu sont assujettis aux conditions présentées dans le site

<https://publications-cnrc.canada.ca/fra/droits>

LISEZ CES CONDITIONS ATTENTIVEMENT AVANT D'UTILISER CE SITE WEB.

Questions? Contact the NRC Publications Archive team at

PublicationsArchive-ArchivesPublications@nrc-cnrc.gc.ca. If you wish to email the authors directly, please see the first page of the publication for their contact information.

Vous avez des questions? Nous pouvons vous aider. Pour communiquer directement avec un auteur, consultez la première page de la revue dans laquelle son article a été publié afin de trouver ses coordonnées. Si vous n'arrivez pas à les repérer, communiquez avec nous à PublicationsArchive-ArchivesPublications@nrc-cnrc.gc.ca.



Synthesis of highly fluorinated poly(arylene ether)s copolymers for proton exchange membrane materials[☆]

Dae Sik Kim^a, Gilles P. Robertson^a, Michael D. Guiver^{a,*}, Young Moo Lee^b

^a Institute for Chemical Process and Environmental Technology, National Research Council, 1200 Montreal Road, Ottawa, Ont., Canada K1A 0R6

^b School of Chemical Engineering, College of Engineering, Hanyang University, Seoul 133-791, Korea

Received 8 December 2005; received in revised form 9 March 2006; accepted 14 March 2006

Available online 24 March 2006

Abstract

Highly fluorinated poly(arylene ether)s containing sulfonic acid groups meta to ether linkage (SPAЕ), intended for fuel cell applications as proton electrolyte membrane materials, were synthesized by potassium carbonate mediated nucleophilic polycondensation reactions of commercially available monomers: 2,8-dihydroxynaphthalene-6-sulfonated salt (2,8-DHNS-6), hexafluorobisphenol A (6F-BPA), and decafluorobiphenyl (DFBP) in dimethylsulfoxide (DMSO) at 160–170 °C. FT-IR and ¹H NMR were used to characterize the structures. The sulfonate or sulfonic acid contents (SC), expressed as a number per repeat unit of polymer and ranged from 0 to 0.79, were calculated from ¹⁹F NMR. The proton conductivities of acid form membrane increased with SC value and reached 0.103 S/cm at 90 °C for SPAЕ 80. The methanol permeabilities ranged from 7.4 × 10⁻⁷ to 2.2 × 10⁻⁹ cm/s at 30 °C and were lower than those of other conventional sulfonated ionomer membranes, particularly commercial perfluorinated sulfonated ionomer (Nafion).

Crown Copyright © 2006 Published by Elsevier B.V. All rights reserved.

Keywords: Fluorinated poly(arylene ether)s; Proton conductivity; Methanol permeability; Fuel cell

1. Introduction

Proton exchange membrane fuel cells (PEMFC)s and direct methanol fuel cells (DMFC)s are receiving considerable attention as electrical power sources for vehicular transportation, residences and institutions, and portable devices owing to their high efficiency and innocuous waste emission [1]. Perfluoro-sulfonic acid PEMs, such as Du Pont's Nafion membrane, are typically used as the polymer electrolytes in PEMFCs because of their excellent chemical and mechanical stabilities as well as high proton conductivity. However, this ionomer is very expensive, and the operational temperature limit is considered to be about 100 °C or lower because of the deterioration of transport, mechanical and electrochemical properties and loss of proton conductivity due to dehydration [2]. Additionally, a critical drawback of the Nafion[®] membrane associated with its application in DMFCs is its high methanol permeability (~10⁻⁶ cm²/s),

which drastically reduces the DMFC performance due to high methanol cross-over [3]. As a result, considerable efforts have been made in order to reduce methanol permeability while maintaining high proton conductivity.

Among recently developed polymer electrolyte membranes, many sulfonated polymers such as sulfonated derivatives of poly(ether ether ketone), polysulfone, poly(arylene ether sulfone), poly(styrene) and poly(phenylene sulfide) have been developed for fuel cells due to the high proton conductivity of their protonated derivatives, which are easily accessible by simple polycondensations of commercial or readily prepared monomers or by post-modifications of commercially available high performance polymers [4–8]. Our group also reported the synthesis of poly(arylene ether ketone)s and poly(arylene ether sulfone)s of various structures containing sulfonic acid groups [9–12]. Unless carefully designed, sulfonated aromatic polymers generally have a tendency to swell at high humidity and elevated temperature, although the proton conductivities of these membranes in the range of 10⁻² to 10⁻¹ S/cm have been achieved.

To fabricate polymers with low cost, good processability, and high thermal and chemical stability, a series of flu-

[☆] NRCC Publication No. 47873.

* Corresponding author. Tel.: +1 613 993 9753; fax: +1 613 991 2384.

E-mail address: michael.guiver@nrc-cnrc.gc.ca (M.D. Guiver).

orinated poly(arylene ether)s containing sulfonic acid groups were synthesized. Fluorinated poly(arylene ether)s developed for interlayer dielectric materials may be considered to be good candidate materials for the PEM polymer backbone, due to their excellent thermal stability, good mechanical properties, high hydrophobicity and economical price [13,14]. The presence of the perfluorophenylene units in the main chains imparts excellent mechanical strength as well as good thermal and chemical stabilities [15], while the presence of the ether groups imparts flexibility, facilitating their processability. The physical properties of fluorinated poly(arylene ether)s can be modified by introducing different linkage groups (such as ketone, sulfide, sulfone, oxadiazole) into the main chains [16]. Meng et al. synthesized aromatic poly(arylene ether)s containing either sulfonated groups pendant to the main chain, as well as polyphthalazinones with sulfonic acid groups connected to the phthalazinone moiety which are claimed to reduce hydrolytic and oxidative degradation [17–20].

Recently, poly(aryl ether)s containing sulfonic acid groups were prepared by our group from 2,8-dihydroxynaphthalene-6-sulfonated salt (2,8-DHNS-6), 4,4'-biphenol, and 2,6-difluorobenzonitrile (2,6-DFBN) [21]. They show the improved properties such as lower water contents and high proton conductivities (10^{-1} S/cm). 2,8-DHNS-6 is a commercially available and inexpensive naphthalenic diol containing a sulfonic acid side group, which is widely used in dye chemistry. The objective of this study is to investigate a series of partially fluorinated poly(arylene ether) copolymers incorporating the 2,8-DHNS-6 monomer, which contains sulfonic acid groups bonded meta to ether linkage of a naphthalene ring in the polymer. The present series of poly(arylene ether)s copolymers was synthesized via nucleophilic polycondensation of 2,8-DHNS-6 with commercially available monomer decafluorobiphenyl (DFBP). Hexafluorobisphenol A (6F-BPA) was used in the copolymer composition to control the SC. The thermal stability, swelling, proton and methanol transport properties were investigated.

2. Experimental

2.1. Materials

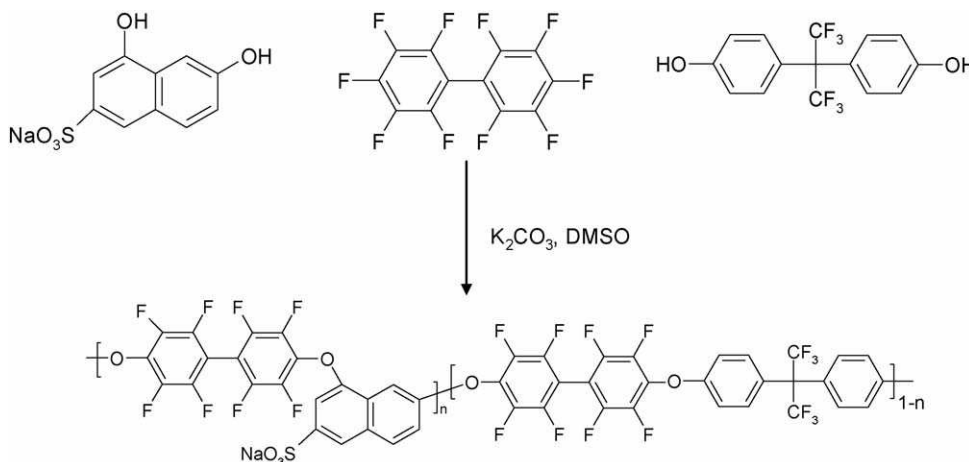
2,8-Dihydroxynaphthalene-6-sulfonated sodium salt (2,8-DHNS-6) was purchased from Rintech, Inc., Maryland, USA and recrystallized from a mixture of ethanol/water (50/50, v/v) before use. Decafluorobiphenyl (DFBP) and hexafluorobisphenol A (6F-BPA) were purchased from Aldrich Chemical Co., USA and was vacuum distilled and purified by sublimation respectively before usage. All other chemicals (obtained from Aldrich) were reagent grade and used as received.

2.2. Copolymerization

The 2,8-DHNS-6 was polymerized with 6F-BPA and DFBP as shown in Scheme 1. A typical synthetic procedure to prepare sulfonated copolymers is described as follows for a target SC of 0.4 (2,8-DHNS-6/6F-BPA = 40/60). 10 mmol DFBP, 4 mmol 2,8-DHNS, 6 mmol 6F-BPA, and 15 mmol K_2CO_3 were added into a three neck flask equipped with a magnetic stirrer, a Dean-Stark trap, and an argon gas inlet. Then, 10 ml DMSO and 10 ml chlorobenzene were charged into the reaction flask under argon atmosphere. The reaction mixture was heated to 130–140 °C. After dehydration and removal of chlorobenzene, the reaction temperature was gradually increased to 160–170 °C. When the solution viscosity had apparently increased, the mixture was cooled to 100 °C and coagulated into a large excess of ethanol or water with vigorous stirring. The precipitated copolymer was washed several times with water and dried in a vacuum oven at 90 °C for 24 h. The resulting polymer was designated SPAE 40, (n) 40 refers to the DHNS molar content of aromatic phenol monomers.

2.3. Copolymer analysis and measurement

IR spectra were measured on a Nicolet 520 Fourier transform spectrometer with membrane film samples in a diamond cell. 1H



Scheme 1. Synthesis of SPAE copolymers.

NMR and ^{19}F NMR spectra were obtained on a Varian Unity Inova NMR spectrometer operating at a proton frequency of 399.95 MHz. Deuterated dimethyl sulfoxide ($\text{DMSO-}d_6$) was the NMR solvent, and the DMSO signal at 2.50 ppm was used as the chemical shift reference.

The degradation process and the thermal stability of the samples were investigated using thermogravimetry (TGA) (TA Instruments, TGA 2950). Polymer samples for TGA analysis were preheated to 200 °C at 10 °C/min under a nitrogen atmosphere and held isothermally for 40 min for moisture removal. The TGA measurements were then carried out under a nitrogen atmosphere using a heating rate of 10 °C/min from 50 to 700 °C.

The bound (non-freezing) and freezing water contents of the SPAE membranes in a fully hydrated state were determined by DSC. A water swollen SPAE membrane was hermetically sealed in a sample pan. The empty sample pan and the sealed pan were weighed, respectively. The sealed pan was quickly frozen inside the DSC chamber to -50 °C and several minutes were allowed for the system to equilibrate. Then, the sample holder assembly was heated up to 50 °C using a heating rate of 2 °C/min. Calculation of the amount of free water in the membrane was done by integrating the peak area of the melt endotherm. The degree of crystallinity of the water, obtained from the heat of fusion of pure water, 334 J/g, was used as a standard [22].

Intrinsic viscosities were determined using an Ubbelohde viscometer for *N,N*-dimethylacetamide (DMAc) solutions of copolymer at 30 °C.

2.4. Preparation of membrane films

An amount of 1 g of copolymer in the sodium salt form was dissolved in 20 ml of DMAc and filtered. The filtered solution was poured onto a glass plate and dried at about 40 °C under a constant purge of nitrogen for about 2 day. The acid form membranes were obtained by immersing corresponding sodium form membranes in 2N H_2SO_4 for 24 h at room temperature and then in deionized water for another 24 h, during which water was changed several times. The thickness of all membrane films was in the range 40–70 μm .

2.5. Water uptake content, ion exchange capacity (IEC) and stabilities

The membranes were dried at 100 °C overnight prior to the measurements. After measuring the weights of dry membranes, the sample films were soaked in deionized water for 24 h at 30 °C temperatures. Before measuring the weights of hydrated membranes, the water was removed from the membrane surface by blotting with a paper towel. The water content was calculated by

$$\text{Water content (\%)} = \frac{W_{\text{wet}} - W_{\text{dry}}}{W_{\text{dry}}} \times 100 \quad (1)$$

where W_{dry} and W_{wet} are the masses of dried and wet samples, respectively.

The ion exchange capacity (IEC, in mmol/g) was determined using the classical titration technique [23].

The oxidative stability of the sulfonated polymers was investigated by immersing the membranes into Fenton's reagent (30 ppm FeSO_4 in 30% H_2O_2) at room temperature, and observing the elapsed time for initial signs of cracking or light bending (t_1) and when the membrane dissolved into solution (t_2).

2.6. Proton conductivity

The proton conductivity measurements were performed on the SPAE membrane by ac impedance spectroscopy over a frequency range of 1–10⁷ Hz with oscillating voltage 50–500 mV, using a system based on a Solatron 1260 gain phase analyzer. A 20 mm × 10 mm membrane sample was placed in a temperature controlled cell open to the air by a pinhole where the sample was equilibrated at 100% RH at ambient atmospheric pressure and clamped between two stainless steel electrodes. The conductivity (σ) of the samples in the longitudinal direction was calculated from the impedance data, using the relationship:

$$\sigma = \frac{l}{RS} \quad (2)$$

where σ is the proton conductivity (in S/cm), l the distance between the electrodes used to measure the potential ($l = 1$ cm), R the impedance of the membrane, and $S (=Wd, W = \text{width}, d = \text{thickness})$ is the surface area required for a proton to penetrate the membrane (in cm^2). The impedance was measured at the frequency that produced the minimum imaginary response.

2.7. Methanol permeability

The permeability experiments were carried out utilizing a glass diffusion cell. One compartment of the cell ($V_A = 100$ ml) was filled with a solution of methanol (10 vol.%) and 1-butanol (0.2 vol.%) in deionized water. The other ($V_B = 100$ ml) was filled with a 1-butanol (0.2 vol.%) solution in deionized water. The membrane (area 1.767 cm^2) was clamped between the two compartments and both of these were kept under stirring during an experiment. A flux of methanol sets up across the membrane as a result of the concentration difference between the two compartments. A detailed description of the experimental set-up and procedure can be found elsewhere [24]. The methanol concentration in the receiving compartment as a function of time is given by

$$C_B(t) = \frac{A}{V_B} \frac{DK}{L} C_A(t - t_0) \quad (3)$$

where C_B and C_A are the two methanol concentrations, A and L the membrane area and thickness, and D and K are the methanol diffusivity and partition coefficient between the membrane and the adjacent solution. The assumptions are made here that D inside the membrane is constant and K does not depend on concentration. The product DK is the membrane permeability. t_0 , also termed time lag, is explicitly related to the diffusivity: $t_0 = L^2/6D$ [25]. C_B is measured several times during an experiment and the permeability is calculated from the slope of the

straight line. Methanol concentrations determined by nuclear magnetic resonance (NMR) spectra were conducted on a Varian Unity Inova 400 NMR spectrometer operating at a resonance frequency of 399.95 MHz for ^1H . For each analysis, solutions were taken directly from the diffusion cell without the use of deuterated solvents. Shimming was done using the ^1H resonance of H_2O . The chemical shift of 1-butanol in D_2O was used as the internal reference standard. During permeability tests the temperature was controlled at 30°C by means of a thermostatic water bath.

3. Results and discussion

3.1. Synthesis and characterization of SPAE copolymers

The conventional synthesis of fluorinated poly(arylene ether)s is usually conducted by a nucleophilic aromatic substitution ($\text{S}_{\text{N}}\text{Ar}$) polycondensation between decafluorobiphenyl compound and diphenol with an excess of anhydrous potassium carbonate [15,26]. As shown in Scheme 1, 2,8-DHNS-6, 6F-BPA and DFBP were polymerized in DMSO and chlorobenzene was used to remove the water from starting materials and formed during the reactions. The polymerization reactions were conducted at $130\text{--}140^\circ\text{C}$, initially to effect dehydration; the reaction temperatures were then raised to 160°C to effect the polymerization, until no obvious further increase in viscosities was observed. Polymerization compositions and properties of polymers are summarized in Table 1. Intrinsic viscosity values of $0.9\text{--}2.1$ dl/g in DMAc at 30°C indicate the success of polymerization in producing high molecular weight polymer. SPAE copolymers with $\text{SC} \leq 0.8$ were obtained, even though polymers containing 2,8-DHNS-6 are expected to be contorted [21]. However, SPAE copolymers with $\text{SC} \geq 0.9$ could not be obtained with high molecular weights. This was probably due to excessive entanglement in the polymer chains that contained fewer linear biphenol segments as well as possibility of branched and even crosslinked polymers. Although the condensation reaction occurs mainly at the para position of the decafluorodiphenyl compounds, giving a linear polymer, it can also occur at the ortho positions, leading to branched and even crosslinked polymers [15].

The structures of the synthesized polymers are also studied by liquid phase ^1H NMR spectroscopy with $\text{DMSO-}d_6$ as the solvent. Fig. 1(a) shows a spectrum of the aromatic protons for the sulfonated copolymer SPAE 50 in sodium form. The bisphenol proton signals H-f, g (2H) appear at low frequencies ($7.2\text{--}7.4$ ppm). The 2,8-DHNS-6 proton signals H-d, e (2H) appear at high frequencies ($8.19, 8.04$ ppm) as observed before in the SPAEEN polymers [21] and the other for H-a, b and c (3H) appear at the frequencies $7.17, 7.9$ and 7.6 cm^{-1} respectively. The restricted mobility of the bulky rigid aromatic chains around the DHNS monomer causes some hydrogen atoms to appear as multiple signals. This is particularly apparent in SPAE 100 where H-a and H-b signals are spread over large spectral windows. Even in SPAE 50 one can see a broad signal for H-b which is affected by the surrounding polymer chains.

Fig. 2 shows fluorine NMR spectra of a series of sulfonated copolymers with different SCs. $\text{DMSO-}d_6$ were used as the solvent with CFCl_3 as the internal reference (0 ppm). The fluorine spectra all show three main signals for every polymer derivatives: F-a (-138 ppm, 4 F), F-b (-153 ppm, 4F) and F-c (-63 ppm, 6F). As shown in Fig. 2, the intensities of the 6F-BPA fluorine signal F-c decreases with increasing SC as a result of replacing 6F-BPA units by DHNS units. The intensities of the fluorine signals arising from the different monomers were used to easily monitor the SC of the copolymers. ^{19}F NMR was preferred to ^1H NMR for measuring SCs since the fluorine signals are well defined and not overlapping unlike ^1H signals. Since the copolymers were prepared by reacting one mole of DHNS and 6F-BPA with one mole of DFBP, the SC is expressed as the ratio of DHNS units (bearing the $-\text{SO}_3\text{Na}$ group) to 1.0 DFBP. Hence, the SC is defined as the number of sulfonic acid salt groups per average repeat unit of copolymer. Having assigned all the ^{19}F NMR signals from the synthetic copolymers, one can use simple mathematical functions and the ratio of spectral line intensities (integral values) to assess the SC. Their integral values were used in the calculation of the SC using the following equation:

$$\text{SC} = 1 - \frac{F_c}{6} \quad (4)$$

Table 1
Composition and properties of SPAE copolymers

Polymer	Content of 2,8-DHNS-6 (mmol)	SC expected	SC from ^{19}F NMR	EW expected g/mol SO_3 (mequiv./g)	IEC measured (mequiv./g)	Td5% ($^\circ\text{C}$)		η_{inh}^c (dl/g)	Oxidative stability ^d (h)	
						Na form	H form ^b		t_1	t_2
SPAE 20	2	0.2	0.18	3077 (0.32)	0.31 (0.30) ^a	486	369	0.9	80	120
SPAE 30	3	0.3	0.27	2027 (0.49)	0.47 (0.46)	471	355	2.1	62	95
SPAE 40	4	0.4	0.38	1501 (0.67)	0.63 (0.61)	464	344	0.72	48	62
SPAE 50	5	0.5	0.48	1187 (0.84)	0.83 (0.81)	451	331	1.5	32	44
SPAE 60	6	0.6	0.57	976 (1.02)	1.00 (0.98)	436	327	0.68	28	38
SPAE 70	7	0.7	0.68	826 (1.2)	1.16 (1.13)	428	314	0.89	24	30
SPAE 80	8	0.8	0.79	714 (1.4)	1.39 (1.37)	424	297	0.82	20	24

^a IEC value after boiling water test for 1 week.

^b Td5% of H form included the loss of bound water.

^c η_{inh} (dl/g) was measured at a concentration of 0.5 g/dl in DMAc for sodium form of SPAE at 30°C .

^d t_1 and t_2 refer to the elapsed time when the membrane began to rupture and when it disappeared in the solution.

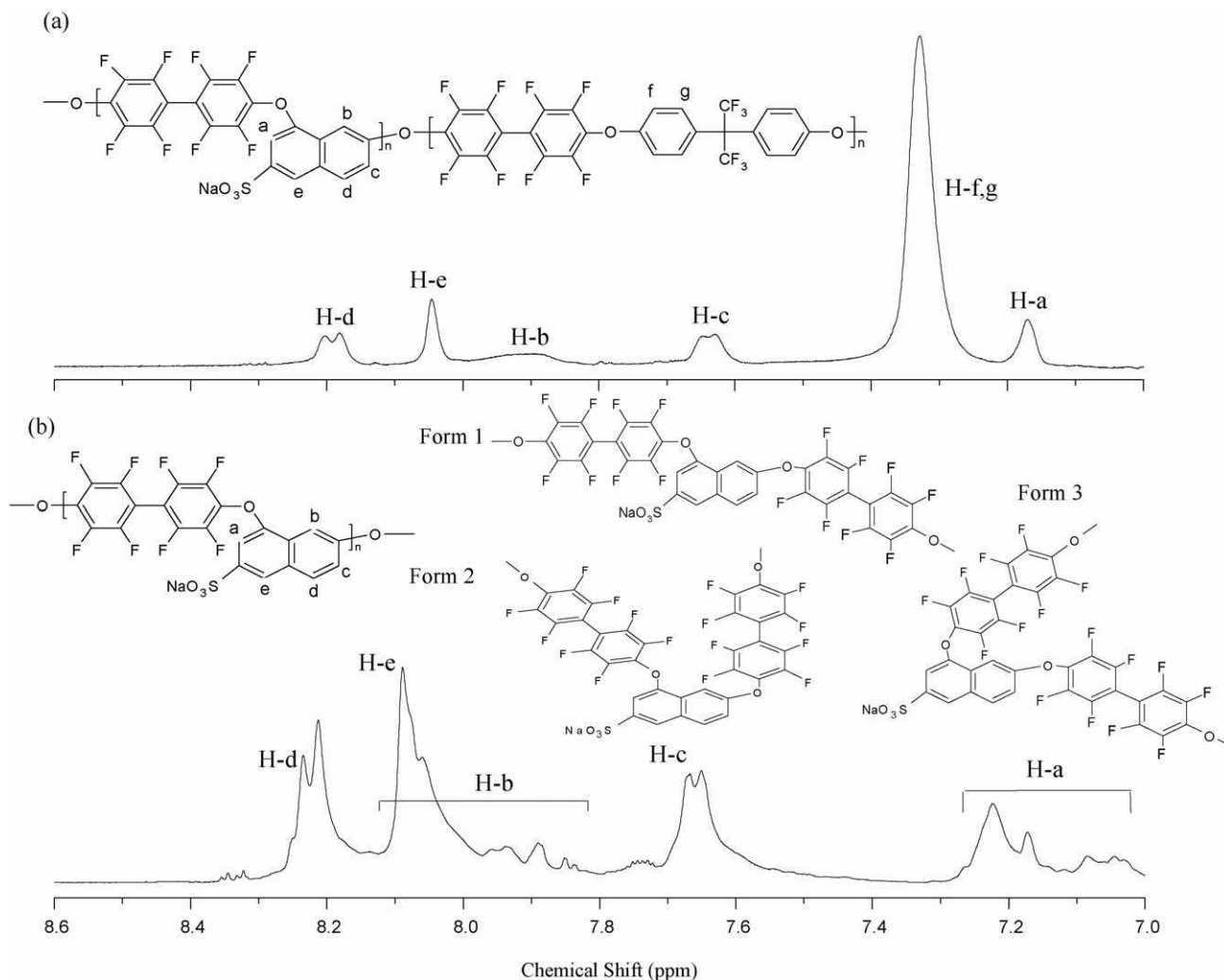


Fig. 1. ^1H NMR spectra of SPAEs in $\text{DMSO-}d_6$ (a) SPAE 50 and (b) SPAE 100.

where Fc is the integral value of F-c after having set the integral values of F-a and F-b to 4F. For example, the spectrum of SPAE 50 shows an integration value of 3.1 for F-c. Inserting this value in the above equations for SPAE 50 results into a SC of 0.48. The observed SC values listed in Table 1. The observed SC values were in agreement with the expected SC derived from the monomer ratios. The restricted mobility of the bulky rigid aromatic chains around the 2,8-DHNS-6 monomer causes some fluorine atoms to appear as multiple signals (marked by arrows) in SPAE copolymers with $\text{SC} \geq 0.6$ as shown in Fig. 2.

The chemical structures of SPAE copolymers are also confirmed by FT-IR as shown in Fig. 3. The IR absorption band at 1008 cm^{-1} is characteristic of the Ar–O–Ar linkage. Characteristic bands of the aromatic sulfonate salt are observed at 1045 and 1084 cm^{-1} and the intensity of these characteristic absorption bands increase with SC which confirm successful introduction of sulfonate groups into polymers.

3.2. Thermal properties of SPAE copolymers

Thermal properties of the membranes were investigated by thermogravimetry programmed from 50 to $700\text{ }^\circ\text{C}$ as shown in

Fig. 4. The copolymers showed only one weight loss step for Na^+ form polymers at around $430\text{--}530\text{ }^\circ\text{C}$ attributed to the degradation of polymer chain. However, three consecutive weight loss steps are observed in the H^+ form polymers. The first weight loss up to $150\text{ }^\circ\text{C}$ is closely associated with the loss of absorbed water molecules that seem to be bound directly to the sulfonic acid group. The second weight loss at around $250\text{--}400\text{ }^\circ\text{C}$ is due to a weight loss of the $\text{--SO}_3\text{H}$ by the desulfonation. In the third weight loss region (at temperature $>450\text{ }^\circ\text{C}$), the polymer residuals are further degraded, corresponding to the thermal decomposition of polymer main chains. The 5 wt.% weight loss temperature ($\text{Td}_{5\%}$) of the membranes is from 424 to $486\text{ }^\circ\text{C}$ in sodium form and from 297 to $326\text{ }^\circ\text{C}$ in acid form as shown in Table 1, indicating good thermal stability.

3.3. State of water in the membranes

Generally, the state of water in the polymer can be classified as free water, freezing bound water and non-freezing bound water [22]. Water molecules strongly associated to ionic and polar sites in the polymer chain are defined non-freezing bound water, and cannot be detected by DSC. In addition, there are two

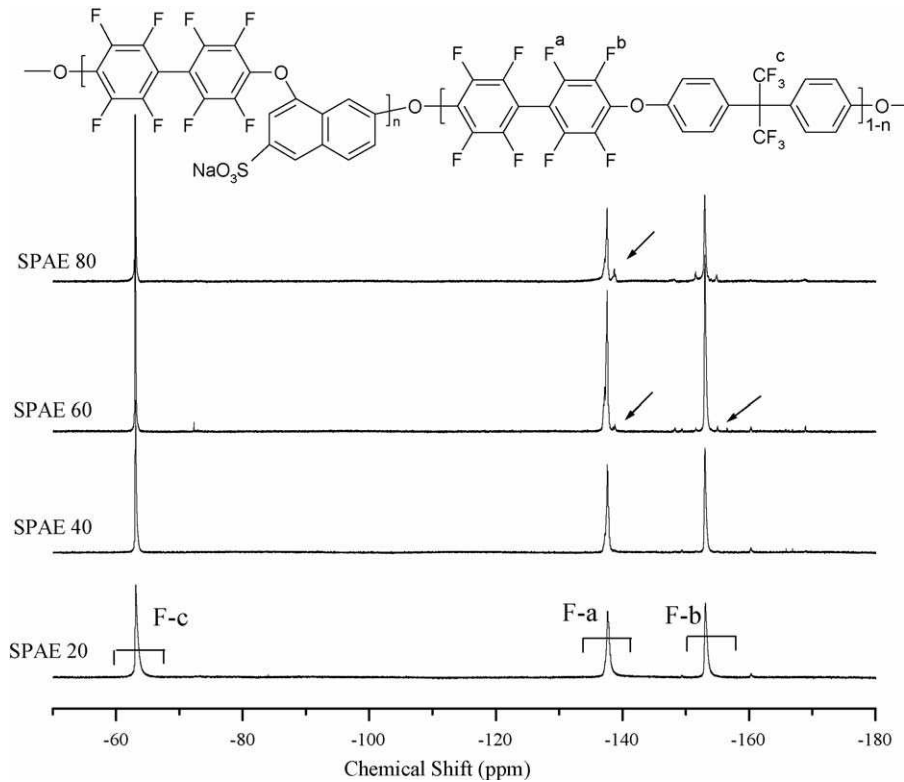


Fig. 2. ^{19}F NMR spectra of SPAE copolymers (the restricted mobility of the bulky rigid aromatic chains around the 2,8-DHNS-6 monomer causes some fluorine atoms to appear as multiple signals (marked by arrows) in SPAE copolymers with $\text{SC} \geq 0.6$).

types of freezing water, namely freezing bound water and free water. Freezing bound water is defined as water that has a phase transition temperature of less than 0°C , and arises from a weak interaction with the polymer and bulk water. The free water is defined as water that has the same phase transition temperature as bulk water (i.e. 0°C), and that is seemingly unaffected by the polymer matrix. It is reported that an important reason for the higher methanol permeability for Nafion is its higher fraction of freezing bound and free water to total water [27]. Generally, a low fraction of free water in membranes leads to a low electroosmotic drag under fuel cell operation, resulting in low methanol

permeabilities [28]. The high bound water content would be an attractive membrane characteristic when employed in DMFCs. Therefore, the study in the state of water in the membranes might be informative. In this study, DSC measurements were used to determine the volume of free water that was not bound by hydrogen bonding.

Fig. 5 shows the typical DSC heating traces of the SPAE and Nafion 117 membranes after being fully swollen. In the SPAE system, the membranes up to $\text{SC} < 0.7$ show the only one endothermic peak corresponding to the freezing water, while

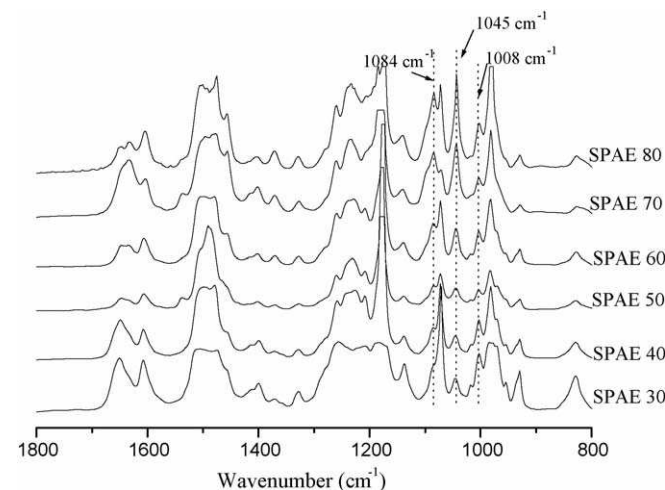


Fig. 3. FT-IR spectra of SPAE copolymers.

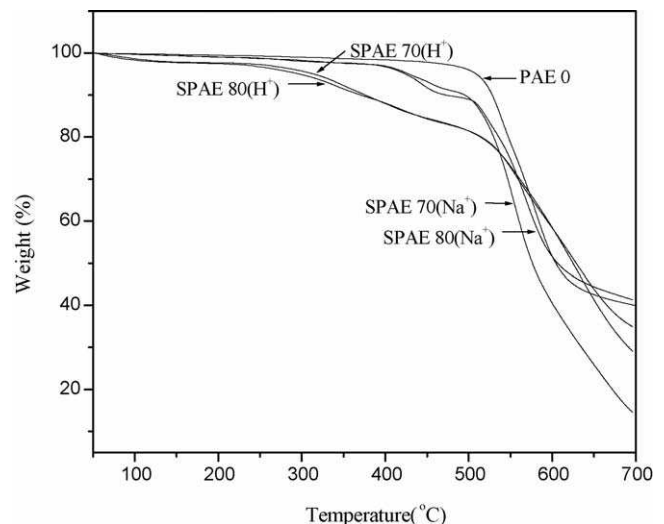


Fig. 4. TGA spectra of SPAE copolymers.

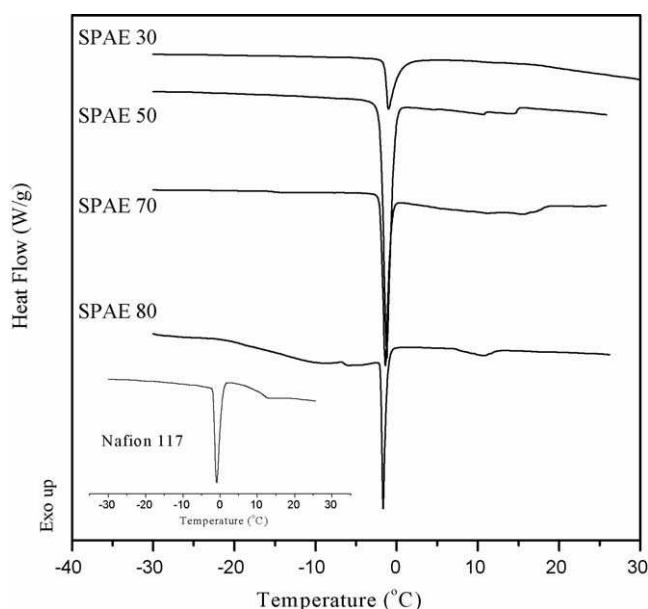


Fig. 5. DSC melting curve of swelling membranes.

the SC > 0.8 (SPAE 80) membrane exhibits two endothermic peaks, suggesting the existence of two states of freezing water. The peak below 0 °C in these membranes corresponds to the melting of freezing bound water, whereas the peak near 0 °C corresponds to the free water. Quantification of each state of water by DSC is obviously of great interest but is difficult because of the two overlapping melting peaks [29]. Therefore, we consider this endothermic peak shown in the DSC results to arise from freezing water (freezing bound water and free water). Table 2 shows the water content corresponding to the freezing water and bound water as well as to the total water contents. The number of water molecules per sulfonic acid group was calculated (λ , mol H₂O/mol SO₃H). Also, the fraction of each state of water and the difference values (Δ) between fraction of freezing water and fraction of bound water are shown in Table 2. The water content of SPAE membranes may be compared with that of Nafion 117 membrane that absorbs water corresponding to about 23 wt.% ($\lambda = 14$ mol H₂O/mol SO₃H). The difference value (Δ) of Nafion 117 (0.49) is higher than that of SPAE mem-

Table 3
Water content and stability of the SPAE membranes

Polymer	Water content (%)		H ₂ O/MeOH (1:1)	
	30 (°C)	80 (°C)	30 (°C)	80 (°C)
SPAE 20	5.3	7.5	8.7	10.5
SPAE 30	8.5	12.6	10.9	16.4
SPAE 40	12.5	15.1	18.1	24.3
SPAE 50	17.0	21.3	21.2	31.5
SPAE 60	23.4	28.5	28.2	45.8
SPAE 70	29.0	35.2	32.5	60.2
SPAE 80	35.5	40.2	38.6	66.5
Nafion 117	23.0	25.6	58.5	98.6

branes (0.22–0.32). The high difference value means that the water molecules exist in the freezing water state rather than in the bound water state. Therefore, the Nafion 117 has higher fraction of freezing water than the SPAE membranes. A high fraction of bound water would be an attractive membrane characteristic when employed in DMFCs [27]. In addition, Table 3 shows the water content in H₂O and H₂O/methanol (50:50 wt.%) in SPAE membranes and Nafion 117 at 30 and 80 °C. Both of the water content increase with temperature. The water content of Nafion 117 in H₂O/methanol is higher than that of SPAE membranes. The results suggest that SPAE membranes have less affinity to methanol than Nafion and it may be advantageous to use SPAE membranes to reduce methanol crossover in a DMFC.

The oxidative stability was investigated by immersion of SPAE membranes into Fenton's reagent at 30 °C and observing the elapsed times for initial (t_1) and final (t_2) membrane degradation. As can be seen in Table 1, all sulfonated membranes exhibited comparable oxidative stabilities to many other sulfonated polymers, but lower than those claimed in references [18,19]. The hydrolytic stability was also investigated by treating membrane in boiling water. The IECs of SPAE membranes before and after boiling water test are listed in Table 1. The SPAE membranes treated with boiling water were less influenced by this treatment than other sulfonated polymers, since the IEC values remained constant even after 1 week of boiling. This result suggests that the SPAE membranes have hydrolytic stability.

Table 2
Characterization of water content in the membranes at 30 °C

Polymer	Water content (%)			λ [H ₂ O]/[SO ₃ H]			Δ^d
	Total	Freezing	Bound	Total	Freezing	Bound	
SPAE 20	5.3	3.5	1.8	9.5 (1) ^a	6.3 (0.66) ^b	3.2 (0.34) ^c	0.32
SPAE 30	8.5	5.5	3.0	10.0 (1)	6.5 (0.65)	3.5 (0.35)	0.29
SPAE 40	12.5	8.0	4.5	11.0 (1)	7.0 (0.64)	4.0 (0.36)	0.28
SPAE 50	17.0	10.7	6.3	11.4 (1)	7.2 (0.63)	4.2 (0.37)	0.26
SPAE 60	23.4	14.9	8.5	13.0 (1)	8.3 (0.64)	4.7 (0.36)	0.27
SPAE 70	29.0	18.1	10.9	13.9 (1)	8.7 (0.62)	5.2 (0.38)	0.25
SPAE 80	35.5	21.6	13.9	14.2 (1)	8.6 (0.61)	5.6 (0.39)	0.22
Nafion 117	23.0	17.1	5.9	14.0 (1)	10.4 (0.74)	3.6 (0.26)	0.49

^a $[\lambda \text{ of total water}]/[\lambda \text{ of total water}]$.

^b $[\lambda \text{ of bound water}]/[\lambda \text{ of total water}]$.

^c $[\lambda \text{ of freezing water}]/[\lambda \text{ of total water}]$.

^d $\Delta = [\text{fraction of freezing water}] - [\text{fraction of bound water}]$ (e.g. Δ of Nafion 117 = 0.74 – 0.26 = 0.49).

3.4. Proton conductivity and methanol permeability

Prior to the proton conductivity measurements, membranes were immersed in boiling water for 2 h and were then soaked in water at 60 °C for 3 days to hydrate. The proton conductivity measurements were run at 100% relative humidity as a function of SC and temperature in the longitudinal direction by AC impedance spectroscopy. Fig. 6(a) shows the complex impedance spectra of the SPAE 70 membrane for different temperature, and additional spectra of SPAE 60–80 at 90 °C. The spectrum is attributed to the capacitance of the membrane acting in parallel with its resistance, and an equivalent circuit was used to obtain the conductivity values [30]. The membrane resistance was considered to be the intersection of the arc with the Z' (Ohm) axis. Increasing temperature leads to smaller semicircles due to reducing resistance because proton conductivity is in general a thermally stimulated process. In addition, the resistance decreased with increasing the 2,8-DHNS-6 mol% due to increasing amount of proton conducting

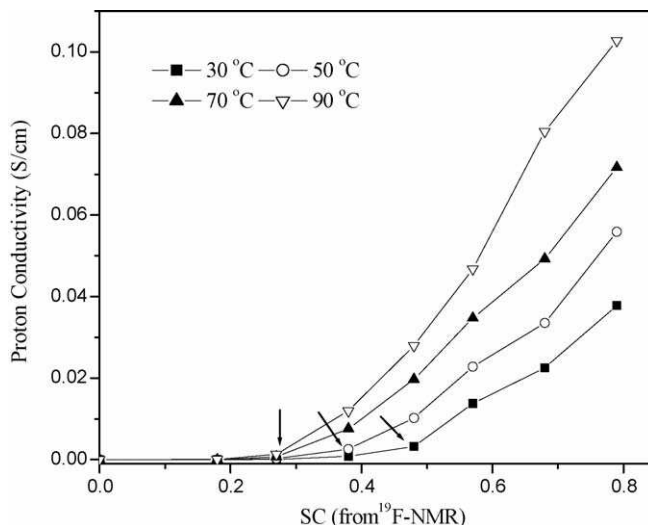


Fig. 7. Proton conductivities of SPAE membranes at different SC. The transition SC of Regimes 1 and 2 are marked by arrows (regimes 1: the proton conductivity only slightly increases with SC; regime 2: the proton conductivity increased rapidly with SC).

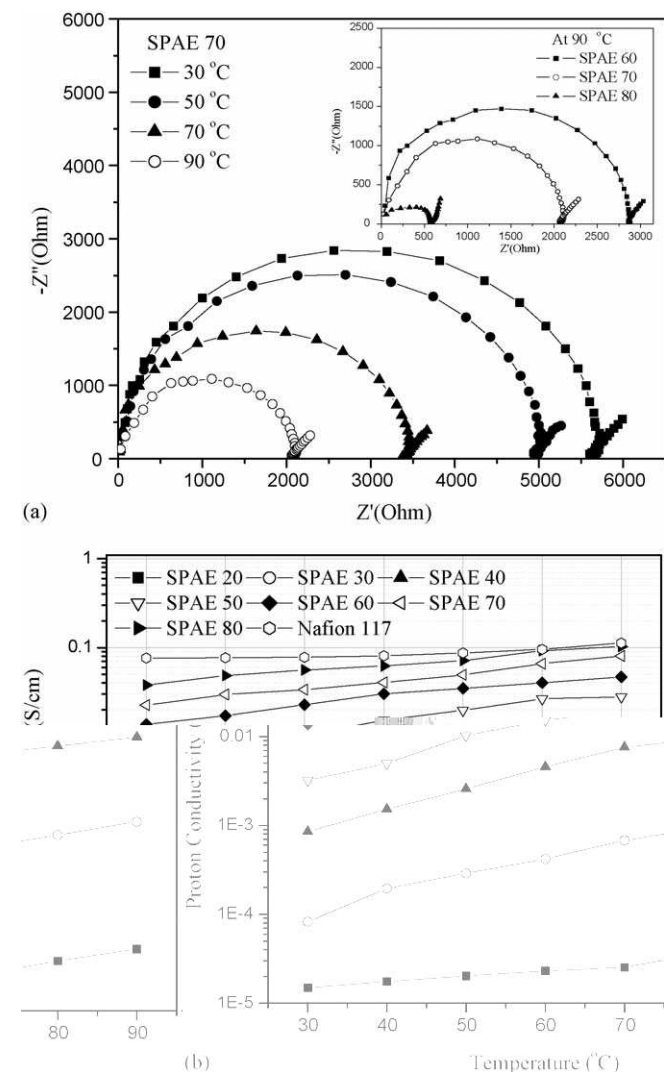


Fig. 6. (a) Complex impedance spectra and (b) proton conductivities of SPAE membranes at different temperatures.

groups ($-\text{SO}_3\text{H}$). Fig. 6(b) shows that the proton conductivities of SPAE membranes increase with both SC and temperature. All SPAE membranes display temperature-dependant proton conductivity curves parallel to that of Nafion 117. As SC increased, the number of hydrophilic domains gradually increased, until finally the water clusters are in close proximity with each other, giving rise to an increase in the proton conductivity. As shown in Fig. 6(b), an increase in SC from 20 to 50 mol% resulted in a two or three orders of magnitude increase in proton conductivity. At SC > 50 mol%, the rate of increase in proton conductivity with SC decreases gradually. Fig. 7 shows the proton conductivities plotted against SC. The proton conductivity results defined two discernable regimes which are dependent on the SC. For example, in Regime 1, the proton conductivity only slightly increases with SC. In Regime 2, the proton conductivity increased rapidly with SC. The transition SC of Regimes 1 and 2 are marked by arrows in the Fig. 7. At low SC values, hydrated sulfonic acid groups form mainly distributed clusters and less connected channels, which resulted in low proton conductivity. The hydrophilic pathway, through which protons could easily pass, may become broader and continuous with increasing SC, thus allowing increased proton conductivity.

The degree of hydration of sulfonated membranes will increase with increasing temperature. In addition, as the proton conductivity of an electrolyte is generally thermally stimulated, it is natural to expect a rise in proton conductivity with temperature [31]. Therefore, the transition SC of Regimes 1 and 2 was lower with increasing temperature. The SPAE 70 and 80 membrane show high proton conductivities comparable with Nafion 117 from room temperature to 90 °C, ranging from 2.2×10^{-2} to 1.03×10^{-1} S/cm. This is explained by taking into consideration the water confinement effect of 2,8-DHNS-6 structure. In a previous study on poly(aryl ether ether nitrile)s prepared from 2,6-difluorobenzonitrile (2,6-DFBN), 4,4'-biphenol(4,4'-BP), and 2,8-DHNS-6, it was proposed that the angled structure

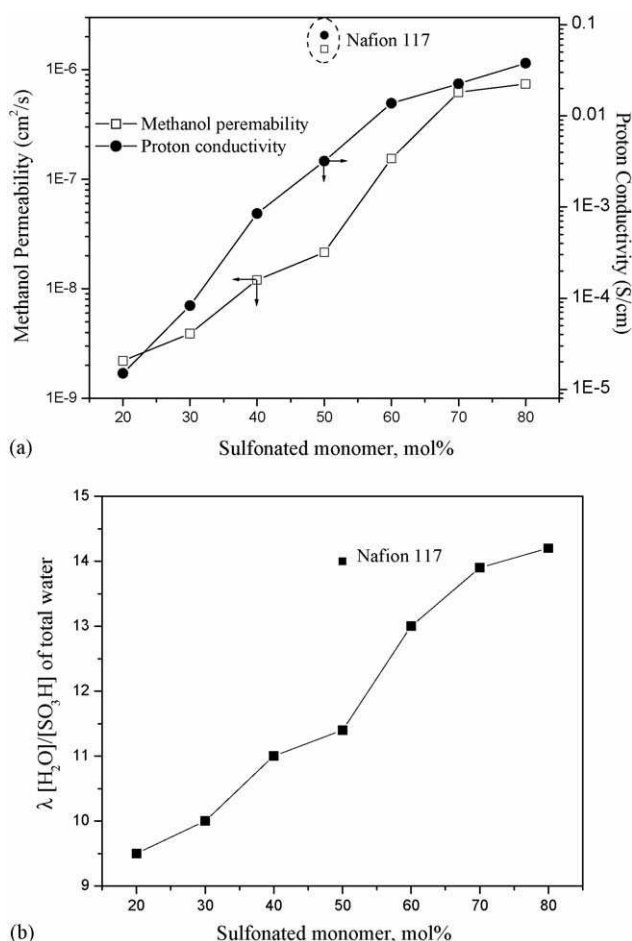


Fig. 8. (a) Methanol permeability and proton conductivity vs. sulfonated monomer content (at 30 °C) and (b) $\lambda \frac{[H_2O]}{[SO_3H]}$ of total water at 30 °C.

of 2,8-DHNS-6 increases the interchain spacing and creates permanent pores lined with $-SO_3H$ group. Once water molecules were absorbed into the pore, these water molecules were bonded with $-SO_3H$ group by hydrogen bond. Using this rationale, the SPAE 70 and 80 membranes show high proton conductivities at even lower temperatures.

Fig. 8(a) shows the proton conductivity and methanol permeability of the SPAE membranes measured as a function of the sulfonated monomer content and Nafion 117. The methanol permeabilities of all the SPAE membranes depended on the sulfonated monomer content, and they were lower than that of Nafion 117 ($1.55 \times 10^{-6} \text{ cm}^2/\text{s}$). The trend in methanol permeability behavior was the same as that observed for the $\lambda \frac{[H_2O]}{[SO_3H]}$ of total water behavior as shown in Fig. 8(b).

There are various factors affecting the methanol permeability such as SC, membrane morphology, hydrophilic domain size and so on. The methanol permeabilities of SPAE 60 membrane were compared with that of Nafion membrane in this study since the SPAE 60 membrane had similar IEC values and total water content compared with Nafion membrane. The methanol permeability of SPAE 60 was lower than that of Nafion 117. As shown in Table 2, the difference value (Δ) of Nafion 117 (0.49) is higher than that of SPAE 60 membranes (0.27). That is, more water molecules in SPAE 60 membrane exist in the bound water

state rather than in the freezing water state, which can hinder methanol transport. Even if the SPAE 80 membrane had higher water content and SC than Nafion 117, the methanol permeability of SPAE 80 membrane was lower than Nafion 117 membrane. From this result, we concluded that the methanol permeability more depended on the freezing water content. Kim et al. have previously reported [24,32,33] that the methanol permeability can be reduced by reducing the free water content of a membrane, while maintaining a high proton conductivity.

4. Conclusion

A series of poly(arylene ether)s containing sulfonic acid groups bonded meta to ether linkage of a naphthalene ring were prepared by aromatic nucleophilic copolycondensation of the decafluorobiphenyl (DFBP) with various amount of 2,8-dihydroxynaphthalene-6-sulfonated salt (2,8-DHNS-6) and hexafluorobisphenol A (6F-BPA). The structure and sulfonate or sulfonic acid content (SC) were determined using ¹H NMR and ¹⁹F NMR, respectively. SPAE copolymers with SC ≤ 0.8 were obtained, even though polymers containing 2,8-DHNS-6 are expected to be contorted. SPAE copolymers with SC values ≥ 0.9 were not obtained in high molecular weight due to the restricted mobility of the bulky rigid aromatic chains around the DHNS monomer. The thermal stabilities of the SPAE membranes were characterized by TGA, which showed that the 5 wt.% weight loss temperature (Td5%) of the membrane is from 424 to 486 °C in sodium form. The difference value (Δ) between fraction of freezing water and fraction of bound water is higher in Nafion 117 than in SPAE membranes. The high difference value means that the water molecules exist in the freezing water state rather than in the bound water state. Therefore, the Nafion 117 has higher fraction of freezing water than the SPAE membranes. The proton conductivities and methanol permeabilities of SPAE membranes with IEC from 0.84 to 1.4 ranged from 2.7×10^{-2} to $1.02 \times 10^{-1} \text{ S/cm}$ at 90 °C and ranged from 2.15×10^{-8} to $7.4 \times 10^{-7} \text{ cm}^2/\text{s}$, respectively.

Acknowledgements

This work was supported by the National Research Council of Canada Fuel Cell program, funded through the Technology and Innovation Research and Development initiative.

Nomenclature

A, L	membrane area and thickness for methanol permeability (cm ² , cm)
C_B, C_A	methanol concentration (mol m ⁻³)
d	membrane thickness
D, K	methanol diffusivity and partition coefficient between the membrane and the adjacent solution
IEC	ion exchange value (mmol/g)
l	distance between the electrodes to measure the potential (cm)

R	impedance of membrane
S	surface area for proton to penetrate through (cm^2)
V_A, V_B	volume of reservoir (ml)
W	membrane width
$W_{\text{wet}}, W_{\text{dry}}$	weight of wet and dry membrane (g)
<i>Greek letter</i>	
σ	proton conductivity (S/cm)

References

- [1] B.C.H. Steele, A. Heinzel, Materials for fuel-cell technologies, *Nature* 414 (2001) 345–352.
- [2] Y.S. Kim, F. Wang, M. Hickner, S. McCartney, Y.T. Hong, W.T. Harrison, A. Azwodzinski, J.E. McGrath, Influence of the bisphenol structure on the direct synthesis of sulfonated poly(arylene ether) copolymers. I., *J. Polym. Sci. Part A: Polym. Chem.* 41 (2003) 2264–2276.
- [3] T. Schults, S. Zhou, K. Sundmacher, Current status of and recent developments in the direct methanol fuel cell, *Chem. Eng. Technol.* 24 (2001) 1223–1233.
- [4] X. Shang, S. Tian, L. Kong, Y.Z. Meng, Synthesis and characterization of sulfonated fluorene-containing poly(arylene ether ketone) for proton exchange membrane, *J. Membr. Sci.* 266 (2005) 94–101.
- [5] P. Genova-Dimitrova, B. Baradie, D. Foscallo, C. Poinignon, J.Y. Sanchez, Ionomeric membranes for proton exchange membrane fuel cell (PEMFC): sulfonated polysulfone associated with phosphoantimonic acid, *J. Membr. Sci.* 185 (2001) 59–71.
- [6] D.S. Kim, H.B. Park, J.Y. Jang, Y.M. Lee, Synthesis of sulfonated poly(imidoaryl ether sulfone) membrane for polymer electrolyte membrane fuel cells, *J. Polym. Sci. Part A: Polym. Chem.* 43 (2005) 5620–5631.
- [7] N. Carrette, V. Tricoli, F. Picchioni, Ionomeric membrane based on partially sulfonated poly(styrene):synthesis, proton conduction and methanol permeation, *J. Membr. Sci.* 166 (2000) 189–197.
- [8] K. Miyatake, E. Shouji, K. Yamamoto, E. Tsuchida, Synthesis and proton conductivity of highly sulfonated poly(thiophenylene), *Macromolecules* 30 (1997) 2941–2946.
- [9] Y. Gao, G.P. Robertson, M.D. Guiver, X. Jian, Synthesis and characterization of sulfonated poly(phthalazinone ether ketone) for proton exchange membrane materials, *J. Polym. Sci. Part A: Polym. Chem.* 41 (2003) 497–507.
- [10] Y. Gao, G.P. Robertson, M.D. Guiver, X. Jian, S.D. Mikhailenko, K. Wang, S. Kaliaguine, Direct copolymerization of sulfonated poly(phthalazinone arylene ether)s for proton-exchange-membrane materials, *J. Polym. Sci. Part A: Polym. Chem.* 41 (2003) 2731–2742.
- [11] Y. Gao, G.P. Robertson, M.D. Guiver, X. Jian, S.D. Mikhailenko, K. Wang, S. Kaliaguine, Sulfonation of poly(phthalazinones) with fuming sulfuric acid mixtures for proton exchange membrane materials, *J. Membr. Sci.* 227 (2003) 39–50.
- [12] Y. Gao, G.P. Robertson, M.D. Guiver, S.D. Mikhailenko, X. Li, S. Kaliaguine, Synthesis of poly(arylene ether ether ketone) copolymers containing pendant sulfonic acid groups bonded to naphthalene as proton exchange membrane materials, *Macromolecules* 37 (2004) 6748–6754.
- [13] A.A. Goodwin, F.W. Mercer, M.T. McKenzie, Thermal behavior of fluorinated aromatic polyethers and poly(ether ketone)s, *Macromolecules* 30 (1997) 2767–2774.
- [14] H.C. Lee, H.S. Hong, Y.M. Kim, S.H. Choi, M.Z. Hong, H.S. Lee, K. Kim, Preparation and evaluation of sulfonated-fluorinated poly(arylene ether)s membranes for a proton exchange membrane fuel cell (PEMFC), *Electrochim. Acta* 49 (2004) 2315–2323.
- [15] J. Ding, F. Liu, M. Li, M. Day, M. Zhou, Fluorinated poly(arylene ether ketone)s bearing pentafluorostyrene moieties prepared by a modified polycondensation, *J. Polym. Sci. Part A* 40 (2002) 4205–4216.
- [16] M.B. Smith, J. March, *March's Advanced Organic Chemistry*, 5th ed., Wiley, New York, 2001, p. 850.
- [17] L. Wang, Y.Z. Meng, S.J. Wang, X.H. Li, M. Xiao, Synthesis and properties of sulfonated poly(arylene ether) containing tetraphenylmethane moieties for proton exchange membrane, *J. Polym. Sci. Part A* 43 (2005) 6411–6418.
- [18] Y.L. Chen, Y.Z. Meng, A.S. Hay, Direct synthesis of sulfonated poly(phthalazinone ether) for proton exchange membrane via N–C coupling reaction, *Polymer* 46 (2005) 11125–11132.
- [19] Y.L. Chen, Y.Z. Meng, A.S. Hay, Novel synthesis of sulfonated poly(phthalazinone ether ketone) used as a proton exchange membrane via N–C coupling reaction, *Macromolecules* 38 (2005) 3564–3566.
- [20] L. Wang, Y.Z. Meng, S.J. Wang, A.S. Hay, Synthesis and sulfonation of poly(arylene ether)s containing tetraphenyl methane moieties, *J. Polym. Sci. Part A* 42 (2004) 1779–1788.
- [21] Y. Gao, G.P. Robertson, M.D. Guiver, S.D. Mikhailenko, X. Li, S. Kaliaguine, Low swelling copoly(aryl ether nitrile)s containing meta sulfonic acid groups for PEM application, *Polymer* 47 (2006) 808–816.
- [22] K. Nakamura, T. Hatakeyama, H. Hatakeyama, Studies on bound water of cellulose by differential scanning calorimetry, *Textile Res. J.* (1981) 607.
- [23] D.S. Kim, H.B. Park, Y.M. Lee, Y.H. Park, Preparation and characterization of PVDF/Silica hybrid membranes containing sulfonic acid groups, *J. Appl. Polym. Sci.* 93 (2004) 209–218.
- [24] D.S. Kim, K.H. Shin, H.B. Park, Y.M. Lee, Preparation and characterization of sulfonated poly(phthalazinone ether sulfone ketone) (SPPEK)/silica hybrid membranes for direct methanol fuel cell application, *Macromol. Res.* 12 (2004) 413–421.
- [25] N. Carrette, V. Tricoli, F. Picchioni, Ionomeric membrane based on partially sulfonated poly(styrene):synthesis, proton conduction and methanol permeation, *J. Membr. Sci.* 166 (2000) 189–197.
- [26] R.J. Cotter, *Engineering Plastic: Handbook of Polyarylethers*, Gordon and Breach Science Publishers S.A., Basel, Switzerland, 1995.
- [27] Y.S. Kim, L. Dong, M.A. Hickner, T.E. Glass, V. Webb, J.E. McGrath, State of water in disulfonated poly(arylene ether sulfone) copolymers and a perfluorosulfonic acid copolymer and its effect on physical and electrochemical properties, *Macromolecules* 36 (2003) 6281–6285.
- [28] M. Ise, K.D. Kreuer, J. Maier, Electroosmotic drag in polymer electrolyte membranes: an electrophoretic NMR study, *Solid State Ionics* 125 (1999) 213–223.
- [29] E. Berlin, P.G. Kliman, M.J. Pallansch, Changes in state of water in proteinaceous systems, *J. Colloid Interface Sci.* 34 (1970) 488–494.
- [30] T. Lehtinen, G. Sundholm, S. Holmberg, F. Sundholm, P. Bjornbom, M. Bursell, Electrochemical characterization of PVDF-based proton conducting membranes for fuel cells, *Electrochim. Acta* 43 (1998) 1881–1890.
- [31] S.M.J. Zaidi, S.D. Mikhailenko, G.P. Robertson, M.D. Guiver, S. Kaliaguine, Proton conducting composite membranes from polyether ether ketone and heteropolyacids for fuel cell application, *J. Membr. Sci.* 173 (2000) 17–34.
- [32] D.S. Kim, H.B. Park, J.W. Rhim, Y.M. Lee, Preparation and characterization of crosslinked PVA/SiO₂ hybrid membranes containing sulfonic acid groups for direct methanol fuel cell applications, *J. Membr. Sci.* 240 (2004) 37–48.
- [33] D.S. Kim, K.H. Shin, H.B. Park, Y.S. Chung, S.Y. Nam, Y.M. Lee, Synthesis and characterization of sulfonated poly(arylene ether sulfone) copolymers containing carboxyl groups for direct methanol fuel cells, *J. Membr. Sci.* 278 (2006) 428–436.